

Arbitrary plasma shape and trapped electron modes in the GEM gyrokinetic electromagnetic turbulence simulation code

Yang Chen, Scott Parker and Jianying Lang

Center for Integrated Plasma Studies, University of Colorado at Boulder, 390 UCB, Boulder, CO 80309

E-mail: yang.chen@colorado.edu

Abstract. Here the recent developments in GEM, a quite comprehensive Gyrokinetic Electromagnetic (GEM) turbulence code are described. GEM is a δf particle turbulence simulation code that has kinetic electrons and electromagnetic perturbations. The key elements of the GEM algorithm are: (1) the parallel canonical formulation of the gyrokinetic system of equations [1]; (2) an adjustable split-weight scheme for kinetic electrons [2]; and (3) a high- β algorithm for the Ampere's equation [3]. Additionally, GEM use a two-dimensional (2D) domain decomposition and runs efficiently on a variety of high performance architectures. GEM is now extended to include arbitrary toroidal equilibrium profiles and flux-surface shapes [4]. The domain is an arbitrarily sized toroidal slice with periodicity assumed in the toroidal direction. It is global radially and poloidally along the magnetic field. Results are presented that demonstrate the effect of plasma shaping on the Ion-Temperature-Gradient (ITG) driven instabilities. An example of nonlinear simulation of the finite- β modified ITG turbulence in general geometry is also given. Finally, collisionless Trapped Electron Modes (TEM) are investigated and shown here is the transition from the TEM dominated core region to the Drift-Wave dominated edge region as the density gradient increases.

1. Introduction

Typically, past gyrokinetic turbulence simulations were carried out for electrostatic ITG driven turbulence with adiabatic ions. Recently, Electron-Temperature-Gradient driven turbulence has also received much attention. In either case, one of the plasma species is assumed to be adiabatic. In the case of ion-Larmor-radius scale ($k_y \rho_i \sim 1$ with $k_y = nq/r$), electromagnetic simulation with fully kinetic electrons poses a number of algorithmic difficulties and has become practical only recently. Here we briefly summarize the GEM algorithm as follows. The gyrokinetic-Maxwell system of equations consists of the gyrokinetic equation for each species, the quasi-neutrality condition for the electric potential ϕ , and Ampere's equation for the vector potential A_{\parallel} . The gyrokinetic equation is written in terms of the canonical momentum $p_{\parallel} = v_{\parallel} + \frac{q}{m} \langle A_{\parallel} \rangle$ as a coordinate [1, 5], to eliminate the inductive component of the electric field $\partial A_{\parallel} / \partial t$ from the equations. To achieve better numerical stability the split-weight scheme is used. Thus the electron distribution is split as $f_e = f_{0e} - \epsilon_g \phi \frac{\partial f_{0e}}{\partial \epsilon_g} + h$, and only the distribution h is represented by the particle weights. Because part of the adiabatic electron response is made explicit in the electron distribution, the rate of change of ϕ , $\dot{\phi} = \partial \phi / \partial t$, is needed to evolve the electron weights.

The equation for $\dot{\phi}$ is derived from the quasi-neutrality condition. Previously we have shown that, to achieve better numerical stability, grid-scale incompatibility between the discretized quasi-neutrality condition and the discretized equation for $\dot{\phi}$ must be introduced [4].

In the typical case of small magnetic skin depth ($k_{\perp}^2 \rho_i^2 \ll \beta_i m_i / m_e$), Alfvén waves are difficult to simulate due to a “cancellation problem” in Ampere’s equation [6]. This problem arises due to a large current carried by the zeroth-order distribution, which is a Maxwellian in terms of p_{\parallel} . This current is largely canceled by an equally large current carried by the distribution h . Because the current from h is computed from the discrete particles, and is subject to discrete particle effects and finite grid-size effects, inexact cancellation can occur if the analytic form of the current from the Maxwellian distribution is used in Ampere’s equation. In the GEM code this problem is solved by also discretizing the Maxwellian term, such that the discrete particle effects and the finite grid-size effects enter the Maxwellian term in the same way as they enter the current from h [3, 4].

These three key elements, the p_{\parallel} formalism, the split-weight scheme and the high- β Ampere algorithm, have been implemented in the GEM code. The simulation domain is an arbitrarily sliced toroidal section of a tokamak, which covers the full poloidal angle ($0 \leq \theta \leq \pi$). The radial domain is typically a significant portion of the minor radius, with a small core region excluded due to the use of field-line-following coordinates, which lead to a singularity at $r = 0$. The field-line-following coordinates (x, y, z) are constructed such that x is aligned with the radial direction, y is the in-surface direction perpendicular to the local magnetic field ($\mathbf{B} \cdot \nabla y = 0$), and $z = q_0 R_0 \theta$ is the direction along the field line. These coordinates allow for efficient representation of the flute-like linear mode structure and the elongated turbulent eddies. The primary dimension for domain decomposition is the z direction. Field equations are solved for each Fourier component in the y direction. The computing of these Fourier components is also fully distributed among the processors at each z grid. Particle pushing is completely distributed among all processors. Thus, the most intensive computations in a particle-in-cell simulation - particle pushing and field solving - are efficiently distributed. A 2D domain decomposition in the z or field-line-following direction and in the x or radial direction is in full production in the flux-tube limit, running efficiently on the IBM SP at NERSC-LBNL and the Cray XT3 at NCCS-ORNL.

2. Effects of flux surface shape on linear spectrum of instabilities

Here we demonstrate the strong effects of flux surface shape on the ITG instability. Electrons are assumed to be adiabatic. The density profile is assumed to be linear with $\rho_i / L_n = 0.0021$. The temperature profile is

$$\frac{T(s)}{T(s_0)} = \exp\left(-\frac{a \Delta s}{L_0} \tanh \frac{s - s_0}{\Delta s}\right) \quad (1)$$

with $s = r/a$, $a = 256.92 \rho_i$, $L_0 = 100 \rho_i$, $s_0 = 0.5$. The q -profile is given by

$$q(s) = 1 + 0.43236s^2 + 2.33528s^3 \quad (2)$$

Other parameters are $m_i / m_p = 1$ (m_p the proton mass), $R_{\text{maj}} = 713.7 \rho_i$, $r_0 = 128.46 \rho_i$. The chosen temperature gradient profile is strongly peaked at s_0 ; hence a relatively small radial domain of $L_x = 90 \rho_i$ is used. Fig. 1 shows the ITG growth rate vs. wave number for both the circular and the shaped equilibria. The equilibrium flux surface shapes are generated from the Miller model [7] with cases (a): $\delta = 0.2$, $\kappa = 1.0$, $R'_0(r) = -0.0$; (b): $\delta = 0.2$, $\kappa = 1.0$, $R'_0(r) = -0.1$ and (c): $\delta = 0.2$, $\kappa = 1.3$, $R'_0(r) = -0.1$. Here δ is the triangularity and κ is the elongation. The results in Fig. 1 show that the ITG instability is generally sensitive to the elongation and the Shafranov shift. The destabilizing effect of the Shafranov shift (compare cases (a) and (b)) is partly due to the fact that the ion temperature profile in the flux label r is fixed. Since the flux surfaces are compressed toward each other on the outer mid-plane, where

the instability tends to localize for ballooning mode structure, a fixed $T_i(r)$ profile has a larger temperature gradient near $\theta = 0$. Both Shafranov shift and elongation shift the instability towards higher toroidal mode numbers, $n = k_y r_0 / q_0$. This feature can be understood as a finite-Larmor-radius (FLR) effect. The perpendicular wave number is given by

$$k_{\perp}^2 = k_x^2 |\nabla x|^2 + k_y^2 |\nabla y|^2 + k_x k_y \nabla x \cdot \nabla y. \quad (3)$$

For a ballooning mode with the ballooning angle $\theta_0 = 0$, $k_x = 0$ at $\theta = 0$; hence $k_{\perp} \approx k_y |\nabla y| \approx \frac{r_0}{q_0} \hat{q}(r, 0) \nabla \theta$. The Shafranov shift reduces k_{\perp} , and hence the FLR stabilization effect, by reducing the local \hat{q} at $\theta = 0$, since a compression of flux surfaces in this region increases the poloidal magnetic field. The elongation, on the other hand, reduces k_{\perp} near $\theta = 0$ through reducing $\nabla \theta$, a geometrical effect.

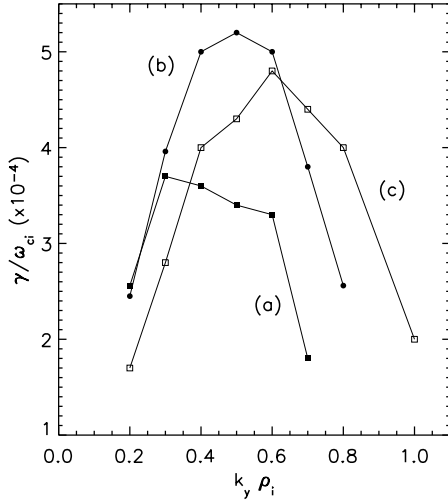


Figure 1. Linear growth rate vs. wave number for (a): $\delta = 0.2$, $\kappa = 1.0$, $R_0'(r) = 0$, (b) $\delta = 0.2$, $\kappa = 1.0$, $R_0'(r) = -0.1$, and (c): $\delta = 0.2$, $\kappa = 1.3$, $R_0'(r) = -0.1$.

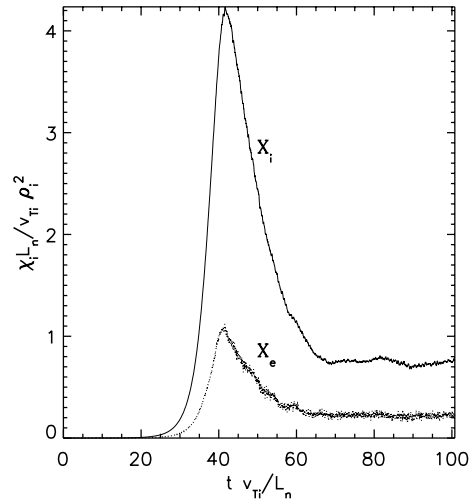


Figure 2. Evolution of ion and electron heat diffusivities.

3. Nonlinear electromagnetic simulation

Here, we use the same q -profile as above. The temperature profiles are given by Eq. 1 with $\Delta s = 0.6$ and $L_0 = 150$. The magnetic surface shape is the same as for case (c) above. Other parameters are: $\beta = 0.012$, $m_p/m_e = 1837$, $L_x = 90\rho_i$, $L_y = 64\rho_i$, $(N_x, N_y, N_z) = (128, 64, 32)$, $\omega_{ci}\Delta t = 2$, 32 particles per cell per species. The split-weight parameter [2] is $\varepsilon_g = 0.5$. The equilibrium parameters at $r = r_0$ are chosen to be close to the Cyclone Base Case [8]: $r/R = 0.18$, $q_0 = 1.4$, $\hat{s} = 0.78$, $R/L_n = 2.2$, $R/L_T = 6.9$. The evolution of the ion and electron heat diffusivities is shown in Fig. 2. The steady state heat diffusivities are $\chi_i = 0.75$ and $\chi_e = 0.22$, in the units of Fig. 2, obtained by averaging over the time window of (70, 100). In flux-tube simulations of the Cyclone Base Case with finite- β we observe that the simulation frequently does not saturate in the long term. For $\beta = 0.01$ without collisions and with a box size of $L_y = 64\rho_i$, flux-tube simulation shows an initial saturation due to the generation of zonal flows. However, the fundamental $k_y \rho_i \sim 0.1$ mode gradually emerges from the zonal-flow modulated

turbulence and continue to grow in the long term, leading to unsaturated streamer transport. Low k_y streamers are not seen in the general geometry simulation of Fig. 2. This is true even with circular, unshifted flux surfaces. In general we find that general geometry simulations behave better in high- β regimes than the flux-tube simulations, and often suggest a weaker finite- β effect on the ITG turbulence than a flux-tube model would suggest.

Our flux-tube simulations at high β , in which low k_y streamers are generated and do not saturate, indicate that the secondary instability, which breaks up a radial streamer at large streamer amplitudes, is weaker in the presence of magnetic field perturbations. This is consistent with observations in flux-tube, fluid simulations [9]. We note, however, that no similar phenomenon is observed at the same β in simulations with the continuum code GYRO [10].

4. Transition from TEM in core plasmas to drift waves in edge plasmas

It is expected that TEM and drift-waves may be important in edge plasmas due to the strong density gradient. Recently, the TEM has been investigated for core plasma parameters [11, 12]. In the core where the density gradient is weak, the drift-waves are stable at low $k_\perp \rho_i$ and can be weakly unstable at larger $k_\perp \rho_i$, but the collisionless TEM is clearly dominant, as seen in Fig. 3, which shows the growth rates vs. k_y for two different density gradients, from flux-tube simulations. Both growth rate scans are normalized to the core value of L_n . The simulations are electrostatic with $\nabla T_e = 0$. Other parameters are $T_e/T_i = 1$, $q = 3$, $\hat{s} = 1$, $r_0 = 200\rho_i$ and $R = 1000\rho_i$. We have tested the dominance of the TEM by zeroing out the trapped electron response and observing no instability at low k . For edge tokamak plasmas the high- k drift wave dominates (see Fig. 3). Simulation of both instabilities requires kinetic treatment of the electrons. The ion response is also important because these modes are on the perpendicular spatial scale of ρ_i . In the simplest case of $\nabla T_i = 0$ (to avoid ITG modes) the coexistence of the TEM modes and drift waves can be readily demonstrated. In the low density gradient case ($\kappa_n \rho_i = 0.01$) the growth rates peak at about $k_y \rho_i = 0.5$, which is identified as a TEM mode. In the high gradient case ($\kappa_n \rho_i = 0.1$) no clear peak is seen in the $k_y \rho_i < 1$ region, where TEM modes are expected to peak. On the other hand, the modes at $k_y \rho_i \geq 1$ can be identified as electron drift waves, which become more unstable as the density gradient increases. Analysis of a shearless slab dispersion relation indicates drift waves are strongly unstable for the representative wave numbers $k_x \approx 0$, $k_\parallel \sim 1/qR$. Turning off the ion response (but retaining the ion polarization term in the Poisson equation) makes the instabilities vanish, consistent with drift wave theory.

5. Summary

The GEM code is a comprehensive gyrokinetic δf particle-in-cell simulation for studying anomalous transport in tokamak plasmas due to electromagnetic microinstabilities. The split-weight scheme is used to increase the time step, which is otherwise limited by the Courant condition due to the fast electron motion. The code features include electron-ion collisions, shaped magnetic flux surfaces, general density, temperature and flow profiles, and an arbitrary number of minority ion species. The effects of flux-surface shaping on ITG modes are demonstrated. Electromagnetic simulations indicate that the finite- β effect on ITG modes is often weaker in global simulations with profile variation than flux-tube simulations suggest. The coexistence of the trapped electron modes and the drift-wave instabilities is shown using electrostatic flux-tube simulations. Transition from the TEM dominated core region, with low density gradient, to the drift-wave dominated edge region, with high density gradient, is observed.

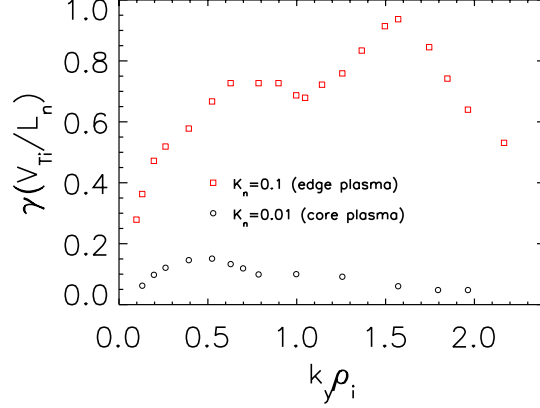


Figure 3. Growth rates vs. $k_y \rho_i$ for typical core and edge density gradients. Both growth rate scans are normalized to the core value of L_n .

Acknowledgments

This work is supported by the DOE SciDAC projects, Gyrokinetic Particle Simulation Center and Center for Plasma Edge Simulation

References

- [1] T. S. Hahm, W. W. Lee, and A. Brizard. Nonlinear gyrokinetic theory for finite-beta plasma. *Phys. Fluids*, 31:1940, 1988.
- [2] Y. Chen and S. E. Parker. Gyrokinetic turbulence simulations with kinetic electrons. *Phys. Plasmas*, 8:2095, 2001.
- [3] Y. Chen and S. E. Parker. A delta-f particle method for gyrokinetic simulations with kinetic electrons and electromagnetic perturbations. *J. Comput. Phys.*, 189:463, 2003.
- [4] Y. Chen and S. E. Parker. Electromagnetic gyrokinetic δf particle-in-cell turbulence simulation with realistic equilibrium profiles and geometry. *J. Comput. Phys.*, in press.
- [5] A.J. Brizard. *Nonlinear gyrokinetic tokamak physics*. PhD thesis, Plasma Physics Lab, Princeton University, 1990.
- [6] J. Cummings. PhD thesis, Plasma Physics Lab, Princeton University, 1994.
- [7] R. L. Miller, M. S. Chu, J. M. Greene, Y. R. Lin-Liu, and R. E. Waltz. Noncircular, finite aspect ratio, local equilibrium model. *Phys. Plasmas*, 5:973, 1999.
- [8] A.M. Dimits, et al. Comparisons and physics basis of tokamak transport models and turbulence simulations. *Phys. Plasmas*, 7:969, 2000.
- [9] B. N. Rogers and J. F. Drake. Enhancement of turbulence in tokamaks by magnetic fluctuations. *Phys. Rev. Lett.*, 79:229, 1997.
- [10] J. Candy. Beta scaling of transport in microturbulence simulations. *Phys. Plasmas*, 12:072307, 2005.
- [11] D. R. Ernst et al. Role of trapped electron mode turbulence in internal transport barrier control in the alcator c-mod tokamak. *Phys. Plasmas*, 11:2637, 2004.
- [12] T. Dannert and F. Jenko. Gyrokinetic simulation of collisionless trapped-electron mode turbulence. *Phys. Plasmas*, 12:072309, 2005.